Title

Proxy-Based VS30 Estimation for Utah Conditioned on Surface Geology and Surface Gradient

Permalink

https://escholarship.org/uc/item/4rp0w60h

Authors

Choi, Joseph
Stewart, Jonathan P
Buckreis, Tristan
et al.

Publication Date

2025-09-06

Proxy-Based V_{S30} Estimation for Utah Conditioned on Surface Geology and Surface Gradient

Joseph Choi[1]; Jonathan P. Stewart, Ph.D., F. ASCE[2];
Tristan E. Buckreis, Ph.D., A.M. ASCE[3]; Scott J. Brandenberg, Ph.D., M. ASCE[3]

[1]Staff Engineer, Earth Mechanics, Inc. Email: j.choi@earthmech.com
[2]Professor, Dept. of Civil and Environmental Engineering, University of California Los Angeles, Los Angeles, CA. Email: jstewart@seas.ucla.edu
[3]Postdoctoral Scholar, Dept. of Civil and Environmental Engineering, University of California Los Angeles, Los Angeles, CA. Email: tristanbuckreis@ucla.edu
[4]Professor, Dept. of Civil and Environmental Engineering, University of California Los Angeles, Los Angeles, CA. Email: sjbrandenberg@ucla.edu

ABSTRACT

The shear-wave velocity profile database was augmented with 259 profiles from 205 unique sites in Utah to facilitate the assignment of site parameters for 95 ground motion recording sites in this region as part of the NGA-West3 project. Three profiles were paired with Utah ground motion stations but 92 other stations lack a co-located profile. A proxy-based model to predict the time-averaged velocity in the upper 30 m of the site (V_{S30}) was developed that considers surface geology and surface gradient for Quaternary units in Utah. The Quaternary surface geologic units considered are Holocene alluvium (Ha), fill (Hf), Pleistocene or undifferentiated Quaternary alluvium (Pa/Qal), alluvium/deltaic (Pad), deltaic (Pd), deltaic-lacustrine or lacustrine (Pdl/Pl), glacial (Pg), undifferentiated Quaternary alluvium - deltaic - eolian (Qa/Qdel/Qe), undifferentiated Quaternary alluvium/deltatic/lacustrine and Holocene deltaic/lacustrine (Qalm/Qdl/Hdl), and lacustrine (Ql). For each unit, V_{S30}-dependence on surface gradient, computed from a digital elevation model with 30 arc-sec resolution, was evaluated and gradient dependencies were identified for 5 of the 11 quaternary units (generally those of Holocene age). The available profile data did not allow the development of models for rock sites, for which V_{S30} was estimated using geology-based models developed for other regions.

INTRODUCTION

Shear-wave velocity (V_S) measures how fast shear waves travel through the Earth. It is also related to the shear modulus of soil as,

$$G_{max} = \rho V_S^2 \tag{1}$$

where ρ is the soil mass density. V_S is a useful site characterization parameter because the speed at which the waves propagate is dependent on the material it passes through. This parameter is commonly used in geotechnical earthquake applications, including for the derivation of a stressstrain backbone curve (this initial modulus is G_{max}) and ground response analyses in which the nature of ground motion change through a profile is dependent on changes in V_S with depth.

Shear wave velocity is also used when no ground response analyses are to be performed but semi-empirical ground motion models (GMMs) are to be applied. The primary parameters used to represent site condition is the time-averaged velocity in the upper 30 m of the site, V_{S30}. The V_{S30} parameter is computed from the V_S profile as the ratio of 30 m to the shear wave travel time from the ground surface to a depth of 30 m.

Typical protocols for V_{S30} assignments (Ahdi et al. 2022) are to use a profile at the instrument site where available. Such estimates carry low uncertainty (typically taken as 0.1 natural log standard deviation; Seyhan et al. 2014). For sites without a measured V_S profile, V_{S30} is estimated using proxy relationships. Such proxy relationships are most useful when they are developed using data from the target region. Relations of this type are available for several regions in the US including California (Wills et al. 2015), central and eastern North America (Parker et al. 2017), and the Pacific Northwest / Cascadia (Ahdi et al. 2017). It is important to develop region-specific models due to regional differences in velocity structure.

Utah is a region of interest due to its high seismic hazard and risk, and consequently, ground motions from Utah are being incorporated in the NGA-West3 database (Buckreis and Stewart 2025). However, no information on site conditions was available in previously NGA databases nor in the shear wave velocity profile database (VSPDB, https://vspdb.org). Using newly acquired V_S profiles located in Utah, a regional V_{S30} proxy model based on slope, geology, and V_{S30} was developed to provide V_{S30} estimates for ground motion stations. Additional details related to the work presented in this paper are provided in Choi (2024).

SHEAR-WAVE VELOCITY DATA IN UTAH REGION

A total of 259 profiles were added to the United States Shear-Wave velocity profile database (VSPDB, https://vspdb.org). Most of the velocity data comes from Utah Geological Survey's (UGS) shear-wave-velocity database (Stephenson et al. 2007), which contains information from a combination of professional engineering reports for projects and research reports. This database contains a total of 253 V_S profiles, which come from 203 distinct sites. Data was also obtained for four additional sites from Wong et al. (2024) and two profiles developed at or near ground motion stations (Cox 2023, Jackson 2024). The velocity data was obtained through multiple measurement methods consisting of downhole, seismic cone penetration testing (SCPT), and surface wave dispersion (including SASW). The available data are mainly from sites located in and near Salt Lake City including the Utah Lake and Great Salt Lake regions.

V_{S30} for each profile was calculated based on available data from the profile based on one of the following conditions:

(1) Computed from a deep profile (maximum depth $\geq$ 30m)
(2) Extrapolated from a shallow V_S profile (maximum depth < 30m) using Dai et al. (2013) model with California-based region-specific coefficients from Kwak et al. (2017)

In some cases, profiles could not be used. This occurred when a profile has insufficient data (e.g., shallowest depth > 5m, deepest depth < 30m) or if no V_S data is available (Vp measurement only)

For profiles with condition (1), V_{S30} was computed using the following equation:

$$V_{S30} = \frac{30m}{\int_0^{30m} \frac{1}{V_S}\, dz} \tag{2}$$

Where V_S is the layer's velocity. For condition (2), a correlation model proposed by Dai et al. (2013) is used to estimate V_{S30},

$$V_{S30} = \frac{30m}{\left(tt_z + \frac{30m - z}{V_{SZ30}}\right)} \tag{3}$$

where V_{SZ30} represents the time-averaged V_S from depth $= z$ to 30 m and tt_z represents travel time from surface to depth $= z$. V_{SZ30} is estimated as,

$$logV_{SZ30} = b_0 + b_1 logV_s(z) \tag{4}$$

The model is derived from a correlation between V_{S30} and $logV_{SZ30}$ developed from datasets from California, Kik-net (Japan), and Turkey (California coefficients were used in the present work). According to a performance evaluation by Kwak et al (2017), Dai et al. (2013) models provided lower model bias and dispersion relative to measured V_{S30} values than other such models.

Approximately 80% of the V_{S30} profiles from Utah are less than 360 m/s, indicating that the data collection was mainly done for soil sites.

SLOPE AND SURFACE GEOLOGY

To compute the topographic gradient, GTOPO30, a 30-arcsec resolution digital elevation model (DEM) provided by USGS's Earth Resources Observation and Science (EROS) center was used (https://www.usgs.gov/centers/eros/science/usgs-eros-archive-digital-elevation-global-30-arc-second-elevation-gtopo30). The use of small cell sizes ultimately was not considered due to past research having found them to be less effective (Allen and Wald 2009).

Surface geologic conditions were obtained from geologic maps sourced from UGS (Utah Geological Survey). A combination of 7.5' and 30' x 60' maps were used, where the 7.5' maps had a resolution of 1:24,000 and the 30' x 60' maps ranged from a resolution of 1:62,000 to 1:100,000.

Once the as-mapped surface geology was identified for each velocity location, initial geologic groupings were made in consideration of the geologic age and depositional environments. Geologic group names were assigned in consideration of age and depositional environment in the case of soil sites and age and rock type in the case of rock sites. When geological conditions were first assessed, 203 of the velocity profile sites were found to be Quaternary in age while only two profile sites are rock sites. The profiles in rock were not considered for this analysis due to data sparseness. Geologic age was split into three groups: (H) Holocene, (P) Pleistocene, and (Q) Quaternary (ambiguous between the Holocene and Pleistocene epochs). Depositional environment was split into eight possible categories: (a) alluvial, (c) colluvial, (d) deltaic, (e) eolian, (f) fill, (g) glacial, (l) lacustrine, or (v) mass-movement. A "mass-movement" depositional environment is a broad category encompassing lateral spread and landslide deposits. With this procedure, a total of 19 geologic groups were formed, with ten groups having five or less measured V_S data. Alluvial and lacustrine depositional environments have the most sites with measured velocities.

GEOLOGY-SLOPE PROXY DEVELOPMENT

Since multiple geologic maps of varying accuracy were used to assess geologic conditions, some of the groups identified may be redundant. To determine if the geologic groups have statistically unique mean V_{S30} values, the natural logarithmic means with error bars indicating ± one standard error of V_{S30} for each geologic group was plotted. Natural logarithmic means were used because V_{S30} has generally been found to be approximately lognormal. Groups Ha, Hf, Pl, and Qa have a small standard error range due to the large number of observations.

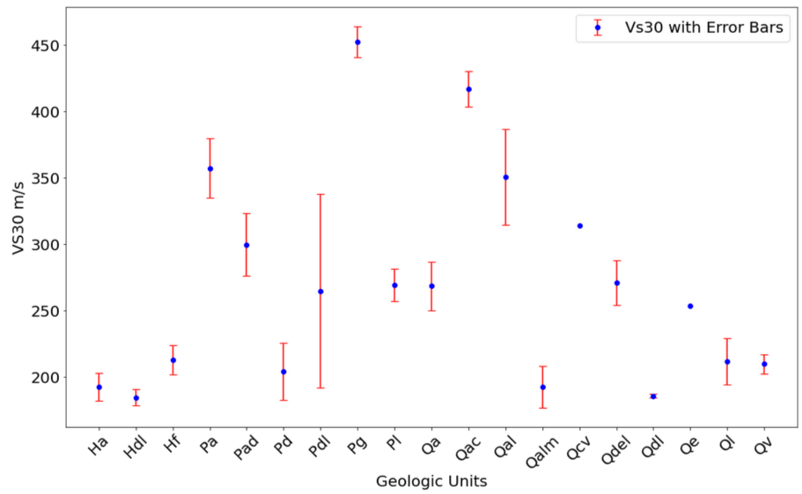

Figure 1. Natural log means for each geologic groups and their standard errors shown as a range.

Where multiple categories have significant overlap of the V_{S30} ranges indicated by the standard error bounds, the null hypothesis that the categories are the same cannot be rejected. We opt to combine these categories, especially if the geologic descriptions are similar. Examples of similar units in Figure 1 are Pa with Qal and Qa with Qdel and Qe. For a more rigorous statistical analysis to see if groups were distinct, F-tests were used. A one-way Analysis of Variance (ANOVA) (Snedecor and Cochran, 1989) was performed to evaluate whether different potential groups (e.g., Pa and Qal) have statistically significant differences. The calculation produces an F_1 statistic as follows:

$$F_1 = \frac{\left[RSS_f - (RSS_1 + RSS_2)\right]/\left[(df_1 + df_2) - df_f\right]}{\sigma^2} \tag{5}$$

in which RSS_f is the residual sum of squares of a data set for a pair of geologic groups, RSS_i is the residual sum of squares for individual group i, df_i is the degree of freedom for model or submodel i (one if the model is mean only and two if the model includes a slope gradient term), and

$$\sigma^2 = \frac{RSS_1 + RSS_2}{N_f - (df_1 + df_2)} \tag{6}$$

Where N_f is the number of data points in the combined data set. The F_1 statistic is compared with the F distribution to evaluate the significance level for the test. If the p-values are < 0.05, the sub-groups exhibit statistically significant differences. The results of the F-tests are shown in Figure 2.

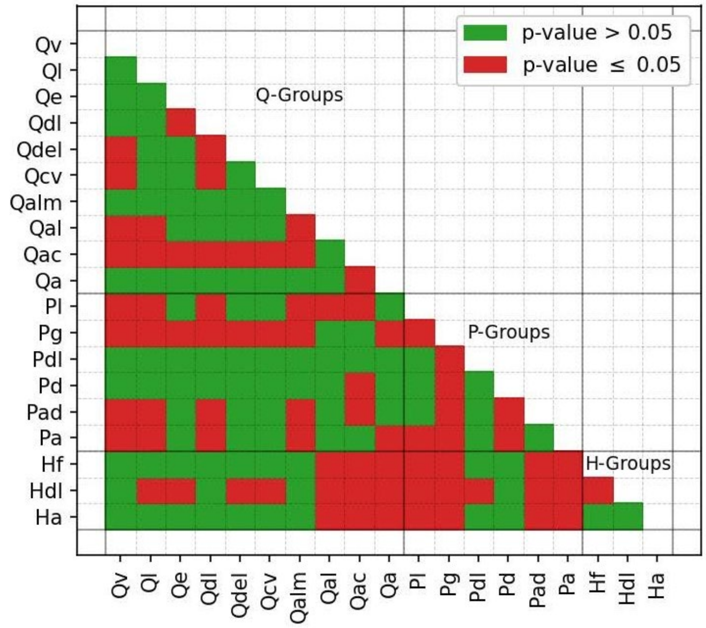

Figure 2. Heatmap showing which combinations of geologic units are distinct (p<0.5) or not distinct (p>0.05) based on the F1 statistic.

The F-tests confirm that fewer than half of the groups have statistically significant differences. The results of the F-tests generally conform with expectations that similar geologic groups are not statistically different (e.g., high p-values observed for Pa/Qal and Pdl/Pl). Using both the binned mean plot and the F-test results, we used judgment to combine geologic groups further from the original 19. In this evaluation, less weight was given to the F-test results when the sample sizes were small (<10), and we only combined groups that we anticipated to likely be similar. This process resulted in 11 groups, five of which represent combinations of groups observed in Figure 1, as follows: Pa/Qal, Pdl/Pl, Qa/Qdel/Qe, Qac/Qcv/Qv, and Qalm/Qdl/Hdl. The final set of geologic groups considered in this research are given in Table 1.

Within the finalized geologic groups, trends between V_{S30} and 30 arc-sec surface gradient were examined using ordinary least squares (OLS) regression in log-log-space,

$$\overline{\ln(V_{S30})} = c_2 + c_3 \ln(s) \tag{7}$$

where V_{S30} has units of meters per second and slope is in meters per meter. A log-log regression was used due to its better visual fit to the data and its lower residual standard deviations compared to a semilog regression. The results of the regression are shown in Figure 3.

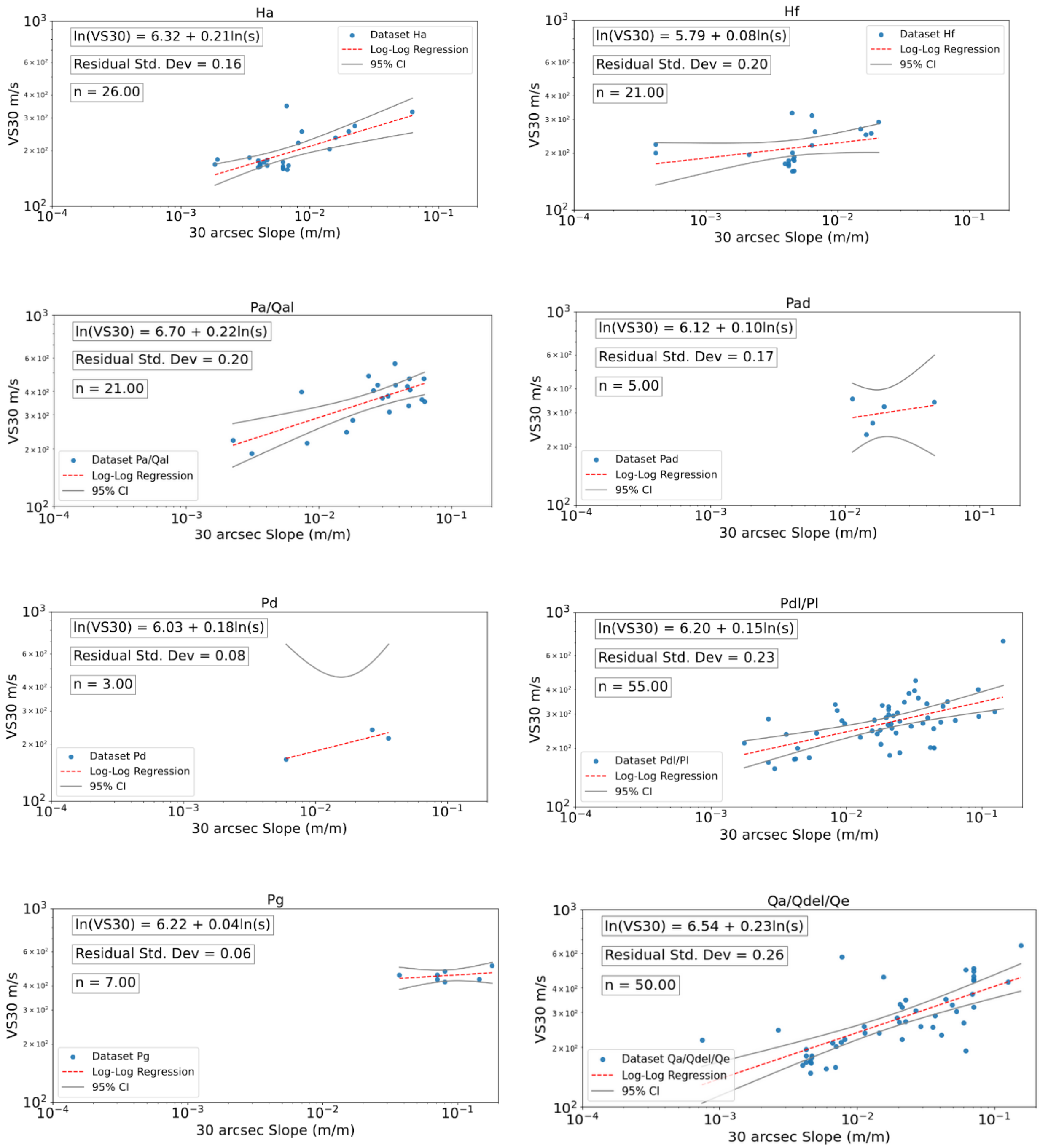

Figure 3. Plots of V_{S30} as a function of slope for all combined geologic groups.

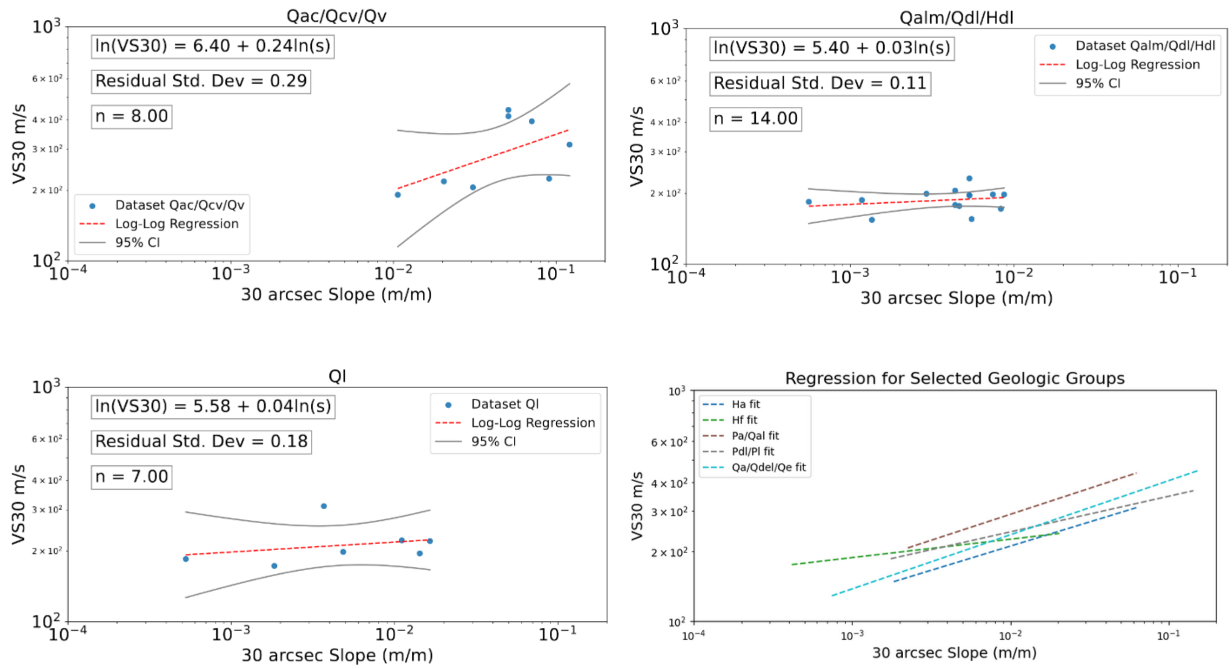

Figure 3 (continued).

If the 95% confidence interval for slope parameter c_3 did not include zero, it was interpreted that slope has a statistically significant effect on V_{S30} and the $\ln(V_{S30})$ mean estimate can be calculated using Eq. 7. The regression results indicate the effects of gradient on V_{S30} exist for only five geologic groupings: Ha, Hf, Pa/Qal, Pdl/Pl, Qa/Qdel/Qe. The finding of gradient dependence of V_{S30} in geologically young units is consistent with V_{S30} proxy models developed in other regions (e.g., Wills et al. 2015, Parker et al. 2017). Gradient dependence was found for different depositional environments, including alluvium, lacustrine, and fill. From visual inspection of Figure 3, it could be argued that all groups but Qalm/Qdl/Hdl and Ql exhibit some trends with slope of varying strength, even though the regression results say otherwise. This is mainly due to the limited data in these geologic groups. Small sample sizes lead to wider confidence intervals thus increasing the likelihood that zero will fall within the interval. It is concluded that while a trend with slope may exist for these units, the available data is insufficient to demonstrate its statistical significance.

To further evaluate the statistical significance of gradient dependence of V_{S30}, the Nash-Sutcliffe Efficiency (NSE) parameter (Nash and Sutcliffe, 1970) was computed for geologic groups Ha, Hf, Pa/Qal, Pdl/Pl, Qa/Qdel/Qe. *NSE* is computed as,

$$NSE = 1 - \frac{\sum_{i=1}^{n}\left(\ln(V_{S30})_i - \overline{\ln(V_{S30})_\mathrm{i}}\right)^2}{\sum_{i=1}^{n}\left(\ln(V_{S30})_i - \mu_{\ln VS30}\right)^2} \quad (8)$$

where $(V_{S30})_i$ is an individual data point, $\overline{\ln(V_{S30})_\mathrm{i}}$ is the gradient-conditioned model prediction (Eq. 7), and $\mu_{\ln VS30}$ is group mean. A value of $NSE < 0$ indicates the regression is a worse predictor than using the mean V_{S30}. As shown in Table 1, *NSE* exceeds zero for the Ha, Hf, Pa/Qal, Pdl/Pl, and Qa/Qdel/Qe groups, showing that Eq. 7 improves over using mean values for these groups.

For the groups that did not exhibit a statistically significant trend with slope, the exponent of the natural log mean of the group is selected to estimate V_{S30}. Table 1 summarizes the geology-slope proxy models proposed to estimate V_{S30} and the recommended coefficients for use in Eq. 7.

Table 1. Summary of proposed V_{S30} estimation models based on geologic conditions and slope

Group	N	Mean V_{S30} (m/s)	Standard Deviation, $\sigma_{\ln V}$	C_2	C_3	Standard Deviation, $\sigma_{\ln V}$	NSE
Ha	26	192.65	0.23	6.32	0.21	0.16	0.48
Hf	21	213.10	0.22	5.79	0.08	0.20	0.14
Pa/Qal	21	345.89	0.28	6.70	0.22	0.20	0.41
Pad	5	299.77	0.18	5.70	0	0.18	-
Pd	3	204.25	0.19	5.32	0	0.19	-
Pdl/Pl	55	269.19	0.27	6.20	0.15	0.23	0.29
Pg	7	452.74	0.07	6.12	0	0.07	-
Qa/Qdel/Qe	49	271.08	0.38	6.54	0.23	0.26	0.49
Qac/Qcv/Qv	8	285.64	0.35	5.65	0	0.35	-
Qalm/Qdl/Hdl	14	187.15	0.11	5.23	0	0.11	-
Ql	7	211.65	0.19	5.35	0	0.19	-

APPLICATION FOR V_{S30} ASSIGNMENTS TO GROUND MOTION SITES

Of the 95 ground motion station sites in the NGA-West3 project, only 3 have a V_{S30} value derived from an on-site profile. For the other 92 sites, the use of proxy-based models are required. This was done using a combination of the regional proxy for Quaternary units (42 sites) and proxies for other regions for rock geologic units (50 sites). For the Quaternary units, the proposed proxy models for V_{S30} estimation are presented in Table 1 and Eq. 7. Due to the lack of measured velocity data for rock sites in Utah, local proxy relationships could not be developed and mean V_{S30} for geologic units of different ages were borrowed from California and central and eastern North America (Wills et al. 2015 and Parker et al. 2017, respectively). Wills et al. and Parker et al. do not provide V_{S30} means for every geologic unit that exists for Utah, which is why both regions were required. Of the 50 stations located on Paleozoic Era rock, one had a co-located V_S profile that was assigned to the station (V_{S30} = 361 m/s).

Figure 4 shows a histogram of the assigned V_{S30} values for the Utah stations. For the rock sites, $\sigma_{\ln V}$ is derived using the standard deviations for the respective units in the source documents (Wills et al. 2015 and Parker et al. 2017) combined with additional epistemic uncertainty as described in Ahdi et al. (2022).

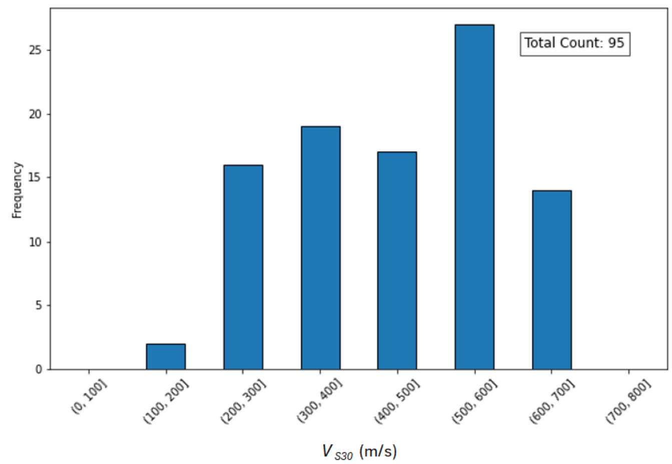

Figure 4. V_{S30} histogram for assigned GMPD ground motion stations.

CONCLUSION

Within the NGA-West3 project, there was a particular need to develop proxy-based models for Utah given the lack of V_S profiles at ground motion recording sites. Based on new profiles added to VSPDB for sites in Utah, a V_{S30} proxy model conditioned on topographic gradient and surface geology was used to assign V_{S30} to ground motion recording sites.

Table 1 presents the developed proxy models for 11 geologic groups. Some geologic groups use a gradient-based relationship while others use the natural log mean of the group. Standard deviations are provided for each V_{S30} estimate. For 42 ground motion stations on soil, proxy models were used to assign V_{S30}. For 50 ground motion stations on rock, V_{S30} was assigned from rock formations in the same era from Wills et al. (2015) and Parker et al. (2017).

REFERENCES

Ahdi S.K., Kwak D.Y., Ancheta T.D., Contreras V., Kishida T., Kwok A.O., Mazzoni S., Ruz F., Stewart J.P. (2022). Site parameters applied in NGA-Sub database. *Earthquake Spectra*, **38(1)**, 494-520.

Ahdi S.K., Stewart J.P., Ancheta T.D., Kwak D.Y., Mitra D. (2017) Development of Profile Database and Proxy-Based Models for Prediction in the Pacific Northwest Region of North America. *Bulletin of the Seismological Society of America 2017*, **107 (4)**, 1781–1801.

Allen T.I., Wald D.J. (2009) On the Use of High-Resolution Topographic Data as a Proxy for Seismic Site Conditions (V_{S30}). *Bulletin of the Seismological Society of America 2019*, **99 (2A)**: 935–943.

Buckreis T.E., Stewart J. P., editors (2025). Data resources for NGA-West3 project. *Report GIRS-2025-xx*, Y. Bozorgnia (PI), B. John Garrick Risk Institute, Natural Hazards Risk and Resiliency Research Center, UCLA (Center Headquarters)

Choi J. (2024). Enhancement of shear wave velocity profile database and application for V_{S30} estimation in Utah. MS Thesis, University of California, Los Angeles.

Cox B.R. (2023). Deep shear wave velocity profiling using MASW and MAM surface wave methods: Valley Emergency Communication Center, Salt Lake City, Utah

Jackson T.S. (2024). Evaluating 1D and 2D small-strain ground response analyses at the I-15 downhole array using recorded aftershocks from the **M**5.7 2020 Magna, Utah Earthquake, *MS Thesis*, Utah State University.

Nash J.E., Sutcliffe J.V. (1970). River flow forecasting through conceptual models Part I – A discussion of principles. *Journal of Hydrology*, **10 (3)**, 282-290.

Parker G.A., Harmon J.A., Stewart J.P., Hashash Y.M.A., Kottke A.R., Rathje E.M., Silva W.J., Campbell K.W. (2017). Proxy-based V_{S30} estimation in Central and Eastern North America. *Bulletin of the Seismological Society of America 2017*, **107 (1)**, 117–131.

Seyhan E., Stewart J.P., Ancheta T.D., Darragh R.B., Graves R.W. (2014) NGA-West2 site database. *Earthquake Spectra*, **30(3)**, 1007-1024.

Snedecor G.W., Cochran W.G. (1989). *Statistical Methods*, Eighth Ed., Blackwell Publishing Professional, Ames, Iowa, ISBN: 978-0-8138-1561-9.

Stephenson W.J., Williams R.A, Odum J.K., and Worley D.M. (2007) Miscellaneous high-resolution seismic imaging investigations in Salt Lake and Utah Valleys for earthquake hazards, *Open-File Report 2007-1152*, U.S. Geological Survey

Utah Geological Survey (2024). Geologic Maps, at https://geology.utah.gov/map-pub/maps/geologic-maps/

Wills C. J., Gutierrez C. I., Perez F. G., Branum D. M. (2015). A next generation V_{S30} map for California based on geology and topography. *Bulletin of the Seismological Society of America*, **105 (6)**, 3083–3091.

Wong I., Darragh R.B., Wu Q., Chowdhury I. (2024). Analyses of site effects in the 2020 **M**5.6 Magna, Utah, Earthquake and development of shallow site amplification factors for Salt Lake Valley, Report to US Geological Survey, NEHRP Grant G22AP00234.